Frontiers in Health Informatics
ISSN-Online: 2676-7104
www.healthinformaticsjournal.com
2024; 13: 03
Open Access

Chronotherapeutic Design of pH-Sensitive Pulsatile Microparticles for Salbutamol Sulphate in Nocturnal Asthma Management

Venkatesh Naik V[1], Ramenani Hari Babu[2], M Deepa[3*], Sarwar Imam[4], Priyanka Vikram Ingle[5], A. Rekha Devi[6], Vema Kiran[7], Touseef Begum[8]

[1]Department of Pharmaceutical Biotechnology, Balaji College of Pharmacy, Affiliated to JNTU Anantapur, Andhra Pradesh -515201.
[2]Department of Pharmacy Practice, Teerthanker Mahaveer College of Pharmacy, Teerthanker Mahaveer University, Moradabad, Uttar Pradesh, India. 244101.
[3]Department of Pharmaceutical Chemistry, Annamacharya College of Pharmacy, Affiliated to JNTU Anantapur, Rajampet -516126 Andhra Pradesh.
[4]Department of Pharmacology, Ambekeshwar Institute of Pharmaceutical Science, Lucknow (U.P) India Pin- 226202.
[5]Department of Pharmacology, Dayanand Education Society's Dayanand College of Pharmacy, Latur Pin-413512.
[6]Department of Pharmaceutics, Seven Hills College of Pharmacy (Autonomous), Venkatramapuram, Tirupati, Tirupati (Dt), Andhra Pradesh, India. PIN-517561.
[7]Department of Pharmaceutics, MB School of Pharmaceutical Sciences, Mohanbabu University, Tirupati, Andhra pradesh-517102.
[8]Ibn Sina National College for Medical Studies, P.O. Box 31906, Jeddah 21418 Kingdom of Saudi Arabia.
Corresponding Author: M Deepa[3*]
Department of Pharmaceutical Chemistry, Annamacharya College of Pharmacy, Affiliated to JNTU Anantapur, Rajampet -516126 Andhra Pradesh.

Cite this paper as: Venkatesh Naik V, Ramenani Hari Babu, M Deepa, Sarwar Imam, Priyanka Vikram Ingle, A. Rekha Devi, Vema Kiran, Touseef Begum (2024) Chronotherapeutic Design of pH-Sensitive Pulsatile Microparticles for Salbutamol Sulphate in Nocturnal Asthma Management. Frontiers in Health Informatics, 13 (3), 5540-5556

ABSTRACT

This study investigates the formulation and evaluation of chitosan-based microparticles designed for controlled drug release, utilizing Salbutamol sulphate as a model drug. Core microparticles were synthesized using a water-in-oil (w/o) emulsion method, incorporating various concentrations of chitosan and Span-85, and subjected to different stirring speeds. Coating of the core microparticles was achieved using Eudragit polymers to develop enteric-coated formulations. The particle size and distribution, morphology, drug entrapment efficiency, loading capacity, and percentage yield were systematically analyzed. Scanning Electron Microscopy (SEM) was employed to assess the surface characteristics of the microparticles, while FTIR and DSC studies were conducted to confirm the chemical compatibility and stability of the formulations. Swelling studies revealed significant insights into the water absorption capabilities of the microparticles. Drug release studies were performed under simulated gastrointestinal conditions, with core microparticles demonstrating varied release profiles across different pH levels. The eudragit coated microparticle did not release the drug in acidic pH of stomach, and the Eudragit S100 and R100 coated microparticle showed burst release at pH 7.4 and at pH 5.8 indicating perfect pH sensitive pulsatile drug delivery. The rapid drug release of certain amount of drug in a short period of time after a lag time makes the system ideal for chronotherapeutic drug delivery system. The pharmacokinetic modeling indicated that MSF-4 had the highest zero-order and Higuchi constants, while EMC-3 showed excellent zero-order fit, highlighting its suitability for sustained release. These findings demonstrated the potential of these microparticles for chronotherapeutic drug delivery, providing a versatile platform for targeted and controlled drug administration.

Keywords: Microparticle, Salbutamol, Chronotherapeutic, Eudragit, Chitosan, pH Dependent.

INTRODUCTION

Chronotherapeutic refers to a clinical practice that involves synchronizing drug delivery with the body's natural circadian rhythms and specific disease states to optimize therapeutic outcomes. This approach aims to maximize health benefits while minimizing potential harmful effects by aligning the timing of medication administration with the body's biological processes. The body's circadian rhythm, which follows a roughly 24-hour cycle, influences various physiological functions, including hormone production, metabolism, and immune response. By considering these natural fluctuations, chronotherapeutic seeks to enhance the efficacy of treatments and reduce side effects. This method is particularly relevant for conditions such as hypertension, asthma, arthritis, and certain cancers, where symptoms and disease activity exhibit daily patterns. Through precise timing, chronotherapeutic can improve drug absorption, distribution, metabolism, and excretion, ultimately leading to better management of chronic diseases and improved patient outcomes (Roy and Shahiwala, 2009). Pulsatile release system is an excellent way for chronotherapeutic drug delivery. Pulsatile release can be described as a fast release of certain amount of drug within a short time period after a lag time (Kikuchi et al., 1999). For chronotherapeutic time controlled system, when a lag time is needed, enteric coated formulation are utilized (Patel and Patel, 2009, Wilding et al., 1994). Physiological activity follows a circadian rhythm, peaking around 4 p.m. and reaching its lowest point around 4 a.m. In individuals with asthma, this circadian fluctuation in lung function can be as much as 50% within a single day. Nocturnal asthma, characterized by the worsening of symptoms during sleep, involves nighttime shortness of breath or wheezing. The intensity of asthmatic attacks is approximately 70 times higher between 4 and 5 a.m. (during typical nighttime sleep) than between 2 and 3 p.m. (during daytime activity). Turner-Warwick reported that among patients undergoing asthma treatment, 94% experienced sleep disturbances at least once a month, 74% once a week, 64% three nights per week, and 39% every night. Codane and Clark found that 68% of asthma-related deaths (13 out of 19 cases) occurred nocturnally, specifically between 12 a.m. and 6 a.m. These findings highlight the critical need for therapeutic strategies that address the time-dependent nature of asthma symptoms, emphasizing the importance of chronotherapy in managing this condition effectively (Aodah, 2009)(Smolensky et al., 2007, Warwick, 1988, Cochrane and Clark, 1975).

Asthma is a chronic respiratory condition characterized by significant circadian variations, with lung function typically reaching its nadir during the early morning hours. This fluctuation can exacerbate symptoms, leading to severe nocturnal asthma attacks that disrupt sleep and increase the risk of morbidity. Salbutamol, a β2-adrenergic agonist, is widely used for its bronchodilatory effects, providing rapid relief from bronchospasm. However, traditional sustained release formulations of Salbutamol often fail to maintain therapeutic blood levels throughout the night, leaving patients susceptible to asthma exacerbations during these critical hours. A chronotherapeutic drug delivery system for Salbutamol aims to address these limitations by aligning drug release with the body's circadian rhythms and the timing of asthma symptomatology. Administering the drug before sleep can ensure that therapeutic levels are sustained from midnight to 8 a.m., the period during which asthma symptoms are most intense. This approach not only improves symptom control but also enhances the patient's quality of life by reducing nocturnal awakenings and the risk of severe attacks. By incorporating a pulsatile release mechanism, the system can deliver an initial dose to provide immediate relief, followed by a sustained release that ensures prolonged protection. This tailored delivery system can optimize the pharmacokinetic profile of Salbutamol, ensuring that drug levels are maintained precisely when needed most. Additionally, this method can reduce the frequency of dosing, thereby improving patient compliance. In conclusion, developing a chronotherapeutic drug delivery system for Salbutamol is a promising strategy to enhance the management of nocturnal asthma. By ensuring sustained therapeutic drug levels during the night, such a system can significantly reduce the incidence of severe asthma attacks, improve patient outcomes, and enhance overall quality of life for asthma sufferers (Soni et al., 2011)(Roy and Shahiwala, 2009, Kikuchi and Okano, 2002)(Bogin and Ballard, 1992). Considering all the above, the present study aimed to develop a chronotherapeutic drug delivery system for Salbutamol for management and treatment of Asthma.

MATERIALS AND METHODS

Materials

Salbutamol sulphate was provided as a gift sample by Remset Pharma, Baddi, India. Chitosan (CS) was obtained from Himedia, India. Eudragit L 100 and S 100 were sourced from Loba Chemicals, Mumbai, India. Light paraffin and glutaraldehyde (GA) were purchased from Sigma Aldrich, Mumbai, India. Span 80, acetone, and petroleum ether were also procured from Sigma Aldrich, Mumbai, India.

Methods

Preparation of Core microparticle

The microparticles were synthesized utilizing a method previously documented in the literature. Initially, a 25% w/v chitosan solution in 1% v/v aqueous acetic acid was prepared, containing Salbutamol sulphate. This dispersed phase was introduced into a continuous phase comprising 125 ml of liquid paraffin with 1% w/v Span-85. The mixture was subjected to continuous stirring to form a water-in-oil (w/o) emulsion. The stirring was maintained at 1500 rpm using a three-blade propeller stirrer for 2.5 hours. Subsequently, a measured quantity (2.5 ml each) of toluene-saturated glutaraldehyde (2.5% w/v) was gradually added to the formed microparticles. The resulting core chitosan microparticles were isolated by centrifugation at 1000 rpm for 30 minutes. The oil and any unreacted glutaraldehyde were completely removed by washing with petroleum ether. The microparticles were then filtered under vacuum and dried. The formulation variables included the concentration of chitosan (drug to polymer ratio) at levels of 1:1, 1:2, 1:3, 1:4, and 1:5, as well as the concentration of the emulsifier Span-85 at 0.5, 1.0, 1.5, and 2.0% w/v. Additionally, the stirring speeds were varied at 1000, 2000, 3000, and 4000 rpm (Umadevi et al., 2010, Gao et al., 2011, Liu et al., 2007, Dhawan et al., 2004).

Table 1. Formulation table showing the composition of the formulations

Formulation Code	Chitosan Concentration (Drug to Polymer Ratio)	Span-85 Concentration (% w/v)	Stirring Speed (rpm)	Continuous Phase Volume (ml)	Emulsification Time (hours)	Glutaraldehyde Quantity (ml)	Glutaraldehyde Concentration (% w/v)
MSF-1	1:1	0.5	500	125	2.5	2.5	2.5
MSF-2	1:1	1.0	1000	125	2.5	2.5	2.5
MSF-3	1:1	1.5	1500	125	2.5	2.5	2.5
MSF-4	1:1	2.0	2000	125	2.5	2.5	2.5
MSF-5	1:2	0.5	1500	125	2.5	2.5	2.5
MSF-6	1:3	1.0	1500	125	2.5	2.5	2.5
MSF-7	1:4	1.5	1500	125	2.5	2.5	2.5
MSF-8	1:5	2.0	1500	125	2.5	2.5	2.5

Coating of the CS-microparticle

The coating process for the CS-microparticles involved the following steps. Initially, Eudragit in different ratios, as detailed in Table 1, was dissolved in 10 ml of an organic solvent mixture comprising acetone and ethanol in a 2:1 ratio. The optimized batch of chitosan core microparticles was then dispersed in this solution. The organic solvent dissolved the Eudragit polymer while preserving the integrity of the chitosan core microparticles. This resulting solution was subsequently poured into 70 ml of liquid paraffin containing Span 80, which was stirred at 1500 rpm for 3 hours at room temperature to facilitate the evaporation of the solvent. Afterward, the coated microparticles were washed with n-hexane to remove any residual petroleum ether. Finally, the microparticles were dried at 30°C for 24 hours (Umadevi et al., 2010).

Determination of mean particle size and particle size distribution

The determination of mean particle size and particle size distribution of both unloaded and drug-loaded microspheres was carried out using optical microscopy with a compound microscope. Initially, a small quantity of the drug microspheres was suspended in 10 ml of purified water. This suspension was then

subjected to ultrasonication for 5 seconds to ensure proper dispersion of the microspheres. A small drop of the resulting suspension was placed on a clean glass slide. The slide was then mounted on the stage of the microscope. The Feret's diameter of at least 300 particles was measured using a calibrated ocular micrometer to ensure accuracy and reliability in the particle size analysis.

Determination of Uniformity Index

The determination of the Uniformity Index (UI) of the microspheres involved several precise steps to ensure accuracy and reliability. Initially, a small quantity of both unloaded and drug-loaded microspheres was suspended in 10 ml of purified water. This suspension was subjected to ultrasonication for 5 seconds to achieve uniform dispersion of the particles. A small drop of the ultrasonicated suspension was then placed on a clean glass slide and mounted on the stage of a compound microscope. Using a calibrated ocular micrometer, the Feret's diameter of at least 300 individual particles was measured to obtain a comprehensive dataset. The mean particle size and standard deviation were calculated from these measurements. The Uniformity Index was then calculated using the formula:

$$UI = \frac{D_w}{D_n}$$

Where D_w and D_n are weight average diameter and number average diameter respectively and are calculated as follows

$$D_w = \frac{\sum D_i N_i^4}{\sum D_i N_i^3}$$

$$D_n = \frac{\sum N_i D_i}{\sum N_i}$$

Where N_i is the number of particles with D_i diameter. Values of *UI* ranging from 1 to 1.1 and 1.1 to 1.2 indicate monodisperse and nearly monodisperse particles. The values higher than 1.2 have been regarded as indicative of particles with broad particle size distribution (Dubey and Parikh, 2004, Shukla et al., 2002).

Morphology study of microspheres

The morphology of the microspheres was studied using Scanning Electron Microscopy (SEM) with the model JSM-5610 from Tokyo, Japan. An appropriate sample of microspheres was carefully mounted on metal (aluminum) stubs using double-sided adhesive tape. To prepare the samples for SEM analysis, the microspheres were fractured with a razor blade to expose their internal structure. Next, the samples were sputter-coated with a thin layer of gold/palladium. This coating process lasted for 120 seconds at a current of 14 mA under an argon atmosphere, which is necessary to enhance the secondary electron emissive properties of the microspheres. The coated samples were then examined using the SEM at an acceleration voltage of 15 kV. The surface morphology and shape of the microspheres were observed at various magnifications to gain detailed insights into their structural characteristics. This method allowed for a comprehensive analysis of the microsphere morphology.

Determination of drug entrapment, loading capacity (LC)

The amount of Salbutamol sulphate present in the microspheres was determined through a meticulous extraction process. Initially, 50 mg of the crushed and powdered microspheres was taken and stirred in distilled water for 15 minutes at 1500 rpm to ensure thorough extraction of the drug. After the extraction, the solution was filtered to remove any particulate matter. The filtrate was then diluted with 0.05 M NaOH to ensure accurate measurement. The absorbance of the diluted solution was measured spectrophotometrically at 276 nm using a UV-Vis 1601 spectrophotometer from Shimadzu. The concentration of Salbutamol sulphate in the microspheres was then determined by employing the simultaneous equation method. This procedure provided a reliable quantification of the drug present in the microspheres, allowing for the calculation of drug entrapment efficiency and loading capacity. The drug entrapment efficiency (EE) was calculated using the formula: EE (%) = (Amount of drug in microspheres / Total amount of drug added) × 100. The loading capacity (LC) was determined using the formula: LC (%) = (Amount of drug in microspheres / Total weight of microspheres) × 100. These calculations provided essential data on the formulation's effectiveness, reflecting the percentage of the initial drug that was successfully entrapped within the microspheres and the percentage of the microspheres' total weight that was composed of the drug (Pachuau and Mazumder, 2009, Jose et al., 2011).

Percentage yield

The percentage yield of the microspheres was determined to assess the efficiency of their production process. Initially, the total weight of all starting materials used in the formulation of the microspheres was recorded. Once the microspheres were formed and dried, they were carefully collected and weighed to obtain the actual yield. The percentage yield was then calculated using the formula:

$$\%\ Yield = \frac{Dried\ microsphere}{drug\ (mg) + chitosan\ weight + \ cross\ linker\ weight}$$

This assessment of percentage yield is crucial for evaluating the success and efficiency of the microsphere preparation process in pharmaceutical and research applications

FTIR Spectroscopy and DSC Thermogram

FTIR (Fourier Transform Infrared Spectroscopy) and DSC (Differential Scanning Calorimetry) thermograms were employed to characterize the microspheres comprehensively to study possible interaction and compatibility. FTIR spectroscopy was conducted to analyze the chemical bonds and functional groups present in the microspheres. A physical mixture of chitosan, Salbutamol, core and coated microsphere with or without drug was prepared as a thin film or pressed pellet and subjected to FTIR analysis using a spectrometer equipped with a suitable detector (Perkin Elmer, Model No. 883). The spectra obtained were compared against reference spectra to identify characteristic absorption peaks corresponding to the components of interest, such as polymers or drug molecules. DSC thermography was employed to investigate the thermal behavior and properties of the microspheres. All samples were sealed in a crimped Aluminum pan and heated at a rate 20^0C / min from 70 to 300^0C in an atmosphere of nitrogen gas by passing at a flow rate of 60 ml/min. An empty aluminum pan was used as a reference. This allowed for the detection of phase transitions, melting points, crystallization, and other thermal events, providing insights into the physical stability and compatibility of the microsphere components. Together, FTIR spectroscopy and DSC thermography provided valuable information regarding the chemical composition, structural integrity, and thermal properties of the microspheres, essential for understanding their compatibility.

Swelling ratio studies

The swelling ratio studies of the microspheres were conducted to assess their ability to absorb and retain fluid over time. Initially, the microspheres were immersed in phosphate buffer saline (PBS, pH 7.4) at room temperature for a duration of 24 hours with gentle shaking to simulate physiological conditions. At specific time intervals (0.5, 1, 2, 4, 6, 8, 12, and 24 hours), samples were carefully removed from the PBS solution and rinsed with Milli-Q water to remove any surface-adhered buffer solution. Throughout the immersion period, it was observed that the microspheres remained intact with no visible microscopic pores, and their original shape was retained. After rinsing, the microspheres were blotted dry to remove excess water, and the swollen weight (Wsw) was measured using an analytical balance. The swelling ratio (Esw) was then calculated using the formula:

$$E_{sw} = \frac{(W_{sw} - W_0)}{W_0} \times 100$$

E_{sw} = swelling ratio of microspheres
W_o = Initial dry weight
W_{sw} = weight of swollen Microspheres.

Drug Release Study: Core Microparticle

The drug release study of core microparticles was conducted to evaluate the release profile of Salbutamol sulphate under various pH conditions mimicking different segments of the gastrointestinal tract. Initially, an accurately weighed amount of core microparticles equivalent to 50 mg of Salbutamol sulphate was suspended in 500 ml of dissolution medium. The dissolution was performed using a USP apparatus Type I (basket method) at 37°C, with stirring set at 50 rpm to maintain sink conditions.

The drug release was studied sequentially in different pH media:

1. **Simulated Gastric Fluid (pH 1.2)**: The microparticles were exposed to 0.1N HCl for 2 hours to simulate gastric conditions.
2. **Simulated Duodenum Fluid (pH 4.5)**: Subsequently, the pH of the dissolution medium was adjusted to 4.5 using appropriate buffers to simulate conditions in the duodenum, and the release was monitored for another 2 hours.

3. **Simulated Distal Ileum and Colon (pH 7.4)**: Finally, the pH of the dissolution medium was adjusted to 7.4 to simulate conditions in the distal ileum and colon, and the release study continued for the remaining duration.

During the dissolution study, samples were withdrawn at specified time intervals, and each withdrawal was immediately replaced with an equal volume of fresh dissolution medium to maintain sink conditions. The withdrawn samples were centrifuged at 2000 rpm to separate the microparticles. The supernatant was then filtered through a membrane filter and analyzed spectrophotometrically at 276 nm using a UV-Vis 1601 spectrophotometer from Shimadzu. This method allowed for the assessment of Salbutamol sulphate release from the core microparticles under conditions mimicking different parts of the gastrointestinal tract, providing insights into its potential for controlled release formulations in pharmaceutical applications (Jose et al., 2011).

Drug Release Study: Coated Microparticle

The drug release study of coated microparticles was conducted to evaluate the release profile of a drug under simulated gastrointestinal conditions. Initially, coated microparticles containing 50 mg of the drug were placed in 500 ml of pH 1.2 (0.1 N HCl) dissolution medium for 2 hours to simulate gastric fluid conditions. The dissolution medium was then replaced with pH 5.8 phosphate buffer and incubated for another 2 hours to simulate conditions in the upper small intestine. Following this, the pH of the medium was adjusted to 6.8 by adding Na2HPO4 and the release study continued for an additional 2 hours to simulate conditions in the lower small intestine. Subsequently, the pH of the medium was further increased to 7.4 to simulate conditions in the distal small intestine and colon, and the release study continued for the remaining duration. During the dissolution study, samples were withdrawn at specified time intervals, and each withdrawal was replaced with an equal volume of fresh dissolution medium to maintain sink conditions. The withdrawn samples were then centrifuged to separate the microparticles, and the supernatant was filtered through a membrane filter. The filtered samples were analyzed spectrophotometrically at 276 nm using a UV-Vis 1601 spectrophotometer (Shimadzu) to quantify the amount of drug released. This method allowed for the assessment of the drug release profile from coated microparticles under conditions mimicking different segments of the gastrointestinal tract, providing valuable information on the potential for controlled release formulations in pharmaceutical applications.

Kinetics of drug release from Microparticle

The kinetics of drug release from microparticles were studied using mathematical models to elucidate the underlying release mechanisms and predict the release behavior over time. Several models were applied to analyze the experimental data obtained from cumulative drug release studies: Firstly, the Zero Order Kinetics model describes drug release as a constant rate over time, represented by the equation where the percentage release is directly proportional to time, governed by the zero-order release rate constant (K). Secondly, the First Order Kinetics model expresses drug release logarithmically against time, indicating exponential decay of drug release with a first-order rate constant (K). The Higuchi Equation elucidates drug release through diffusion from a matrix system, showing a square root dependence of drug release on time, with the Higuchi rate constant (K) representing the rate of drug diffusion in the matrix. Lastly, the Korsmeyer-Peppas Equation or Power Law model characterizes drug release as a function of time raised to the power of n, where M_t/M_∞ is the fractional release of drug at time t, K is the release rate constant, and n is the release exponent indicating the mechanism of drug release (diffusion-controlled for $n \leq 0.5$, anomalous transport for $0.5 < n < 1$, and case-II transport for $n = 1$). These models were applied to experimental data obtained from drug release studies conducted in simulated physiological conditions, providing insights into the release mechanisms and aiding in the formulation and optimization of controlled release systems for pharmaceutical applications.

RESULTS AND DISCUSSION

Stirring speed, determination of mean particle size, particle size distribution and uniformity index

The effect of stirring speed on the formulation can be observed in the formulations MSF-1 to MSF-4, which maintain a constant drug-to-polymer ratio of 1:1 while varying the stirring speed. As the stirring speed increases from 500 rpm to 2000 rpm, the mean particle size decreases significantly from 45.61 µm to 18.41 µm. This reduction in particle size is attributed to the higher shear forces at elevated stirring speeds, which effectively break down the particles into smaller sizes. However, the Uniformity Index (UI) does not

follow a consistent trend with increasing stirring speed. While there is a general improvement in particle uniformity at intermediate speeds, the highest stirring speed (2000 rpm) results in a higher UI, indicating that the uniformity of the particles does not consistently improve with increased speed. The impact of the drug-to-polymer ratio on particle size and uniformity is evident in the formulations MSF-3 to MSF-8, all prepared at a constant stirring speed of 1500 rpm. As the polymer content increases from a 1:1 ratio (MSF-3) to a 1:5 ratio (MSF-8), the mean particle size generally increases from 19.91 µm to 28.31 µm. This increase in particle size with higher polymer content can be attributed to the increased viscosity of the solution, which makes it more challenging to break down the particles during stirring. Concurrently, the Uniformity Index improves significantly, with higher polymer content leading to better uniformity in particle size distribution. For instance, the UI decreases from 2.0869 at a 1:1 ratio to 0.9833 at a 1:5 ratio, suggesting that higher polymer content results in more uniform particle sizes. Coating the particles with Eudragit significantly affects both particle size and uniformity, as seen in the coated formulations ECMSF-1, ECMSF-2, and ECMSF-3. These formulations use different ratios and types of Eudragit coating, resulting in substantial increases in particle size compared to uncoated formulations. For example, ECMSF-1 (Eudragit S 100, 1:10) has a mean particle size of 104.31 µm, while ECMSF-2 (Eudragit S 100, 1:5) and ECMSF-3 (Eudragit L 100, 1:5) have mean particle sizes of 92.31 µm and 92.11 µm, respectively. The increased particle size is expected due to the additional material added by the coating. Moreover, the type and amount of coating influence particle uniformity, with Eudragit S 100 at a 1:10 ratio producing larger particles than at a 1:5 ratio. Additionally, while Eudragit S 100 and Eudragit L 100 at a 1:5 ratio yield similar particle sizes, they exhibit slightly different Uniformity Indices, indicating that the type of Eudragit also impacts particle uniformity (Lorenzo-Lamosa et al., 1998). In summary, optimizing formulation parameters such as stirring speed, drug-to-polymer ratio, and coating material is essential for achieving the desired particle size and uniformity. Higher stirring speeds reduce particle size but do not consistently improve uniformity. Increasing the polymer content generally results in larger and more uniform particles. Coating significantly increases particle size, with the type and amount of coating affecting both size and uniformity. Balancing these parameters is crucial to meet specific formulation goals and ensure the desired characteristics of the final product (Dubey and Parikh, 2004, Jeyanthi et al., 1997).

Table 2. Particle Size Distribution and uniformity index of different formulations.

Formulation	**Drug : Polymer**	**Stirring Speed (rpm)**	**Mean Particle Size(µm)**	**Uniformity Index (UI)**
MSF-1	1:1	500	45.61 ± 5.92	2.181 ± 0.15
MSF-2	1:1	1000	30.11 ± 2.22	2.309 ± 0.10
MSF-3	1:1	1500	19.91 ± 4.52	2.0869 ± 0.14
MSF-4	1:1	2000	18.41 ± 3.62	2.886 ± 0.12
MSF-5	1:2	1500	22.11 ± 0.82	1.1977 ± 0.05
MSF-6	1:3	1500	27.71 ± 0.82	0.995 ± 0.08
MSF-7	1:4	1500	27.91 ± 0.62	0.978 ± 0.05
MSF-8	1:5	1500	28.31 ± 1.62	0.9833 ± 0.12
Coated	**Core: Coat**			
ECMSF-1 (Eudragit S 100)	1:10	1500	104.31 ± 8.92	1.218 ± 0.09
ECMSF-2 (Eudragit S 100)	1:5	1500	92.31 ± 7.02	1.35 ±0.04
ECMSF-3 (Eudragit L 100)	15	1500	92.11 ± 5.22	1.30 ± 0.08

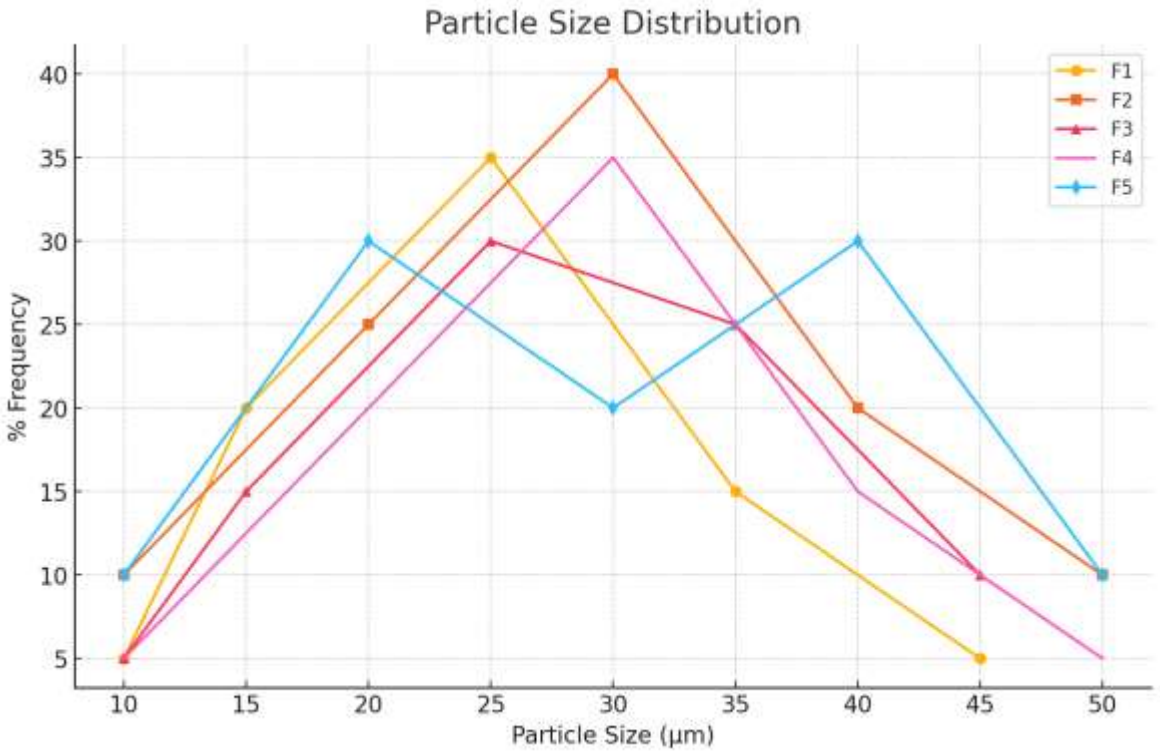

Figure 1. Frequency Destribution of of different formulation.

Morphology study of microspheres

The provided figure shows scanning electron photomicrographs of core microparticles (left) and coated microparticles (right). These images provide a visual comparison of the morphological characteristics of the microparticles before and after coating. The core microparticles (Left Image) in the left image appear to be smooth and spherical. The surface of these particles is relatively uniform with few surface imperfections. The spherical shape and smooth surface suggest a controlled and efficient particle formation process, likely achieved under optimal stirring conditions and appropriate drug-to-polymer ratios. The coated microparticles (Right Image) in the right image exhibit a markedly different morphology. The surface of these particles appears rougher and more irregular compared to the core particles. The coating process has added an additional layer around the core particles, which is visible as a textured and uneven surface. This roughness may result from the coating material adhering and solidifying around the core particles, leading to a more complex surface topology. The differences between the core and coated microparticles highlight the impact of the coating process on particle morphology. The smooth, spherical nature of the core particles is indicative of a well-controlled synthesis process, which is crucial for achieving uniform particle size and shape. The coating, while adding protective or functional layers to the particles, introduces surface roughness and irregularities. This is expected as the coating material envelops the core, often resulting in a less smooth surface. The increased size of the coated microparticles is also evident. The coating layer contributes to the overall diameter of the particles, which is consistent with the data presented earlier, where coated formulations had significantly larger particle sizes compared to uncoated ones. For example, ECMSF-1 with Eudragit S 100 at a 1:10 ratio exhibited a mean particle size of 104.31 µm, significantly larger than the core particles. These morphological changes due to coating can affect the physical and functional properties of the microparticles. For instance, the rough surface might enhance certain interactions with biological tissues or influence the release profile of the encapsulated drug. But as the coating has been a functional modality in this research work to delay drug release, this finding has been fruitful.

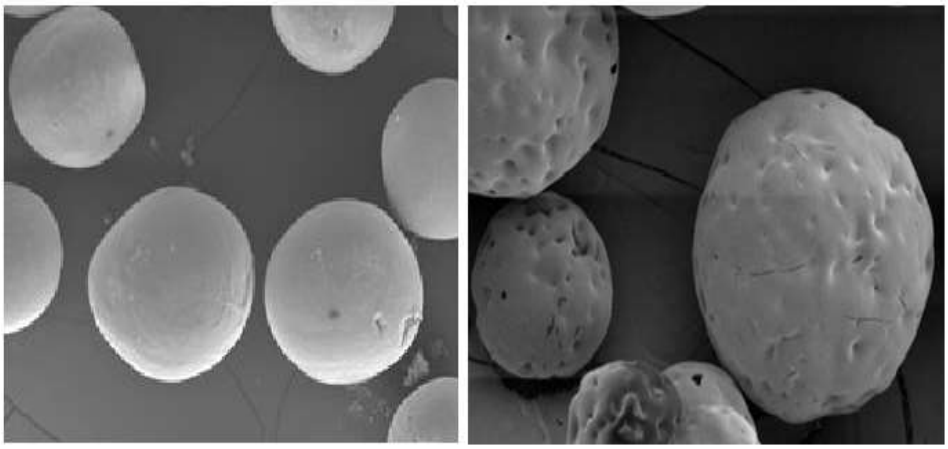

Figure 2. Scanning electron photomicrograph of core microparticle (Left) and coated micro particle (Right).

Encapsulation efficiency, Loading capacity and percentage yield

For formulations MSF-1 to MSF-4, which vary in stirring speed, increasing the speed from 500 to 1500 rpm leads to a gradual increase in both percentage yield and encapsulation efficiency, with the highest values at 1500 rpm. The loading capacity also rises, peaking at 2000 rpm, suggesting that higher stirring speeds enhance drug incorporation per unit mass of microparticles. However, at 2000 rpm, the yield slightly decreases, indicating that very high stirring speeds might introduce inefficiencies or result in particle loss. In formulations MSF-3 to MSF-8, varying the drug-to-polymer ratio shows that higher polymer content (lower drug-to-polymer ratio) results in significantly higher yields, with a peak yield at a 1:4 ratio. This trend suggests improved process efficiency with increased polymer content. However, the loading capacity decreases as the polymer content increases, indicating less drug content per unit mass of microparticles. Conversely, encapsulation efficiency improves with increased polymer content, reaching its highest at a 1:5 ratio, which implies more effective drug entrapment within the polymer matrix. Examining the coated formulations (EMC1, EMC2, and EMC3), it is evident that coating enhances both yield and encapsulation efficiency. All coated formulations exhibit high yields, with EMC2 having the highest at 93.00%. Encapsulation efficiencies are also significantly higher in coated formulations compared to uncoated ones, with EMC3 achieving the highest at 96.47%. The loading capacities across these formulations remain relatively consistent, indicating that coating effectively maintains drug content while significantly improving yield and encapsulation efficiency. In summary, optimizing formulation parameters such as stirring speed, drug-to-polymer ratio, and coating is essential for achieving the desired outcomes in yield, loading capacity, and encapsulation efficiency. Higher stirring speeds generally enhance yield and encapsulation efficiency up to an optimal point, while higher polymer content improves yield and encapsulation efficiency but reduces loading capacity. Coating markedly improves encapsulation efficiency and yield, demonstrating its effectiveness in enhancing drug entrapment and process efficiency.

Table 3. Percentage yield, Loading Capacity and Encapsulation efficiency of different formulation.

Formulation	Rotation Speed (R.P.M)	% yield	Loading capacity (%)	Encapsulation (%)
MSF-1	500	74.33 ± 0.48	25.67 ± 0.261	73.67 ± 0.771
MSF-2	1000	76.03 ± 0.39	26.67 ± 0.351	75.97 ± 0.661
MSF-3	1500	77.11 ± 0.95	27.99 ± 0.321	80.05 ± 0.851
MSF-4	2000	74.03 ± 0.79	29.67 ± 0.431	80.69 ± 0.681
MSF-5	1500	81.12 ± 0.41	19.43 ± 0.301	81.37 ± 0.991
MSF-6	1500	86.59 ± 0.38	14.21 ± 0.071	81.37 ± 0.701
MSF-7	1500	92.18 ± 0.66	11.23 ± 0.851	87.67 ± 0.761
MSF-8	1500	90.74 ± 0.66	9.33 ± 0.211	90.39 ± 0.571

EMC1	1500	90.96 ± 0.89	11.17 ± 0.171	93.71 ± 0.471
EMC2	1500	93.00 ± 0.28	11.69 ± 0.071	96.13 ± 0.571
EMC3	1500	92.02 ± 0.45	11.65 ± 0.191	96.47 ± 0.051

FTIR Study and DSC Thermogram

The FTIR and DSC studies conducted to evaluate the compatibility between the drug and excipients (chitosan, Span-85, and glutaraldehyde) in the microsphere formulation revealed no significant interactions. The FTIR spectra of the physical mixtures and the final formulation showed no major shifts, disappearance, or appearance of new peaks compared to the spectra of the pure drug and excipients, indicating that the chemical structures remained intact and no new bonds were formed. Similarly, the DSC thermograms demonstrated that the characteristic thermal events of the drug and excipients were preserved in the physical mixtures and the final formulation, with no significant changes in melting points or the appearance of new thermal events. These results confirm the absence of any notable interactions between the drug and the excipients, indicating good compatibility within the microsphere formulation.

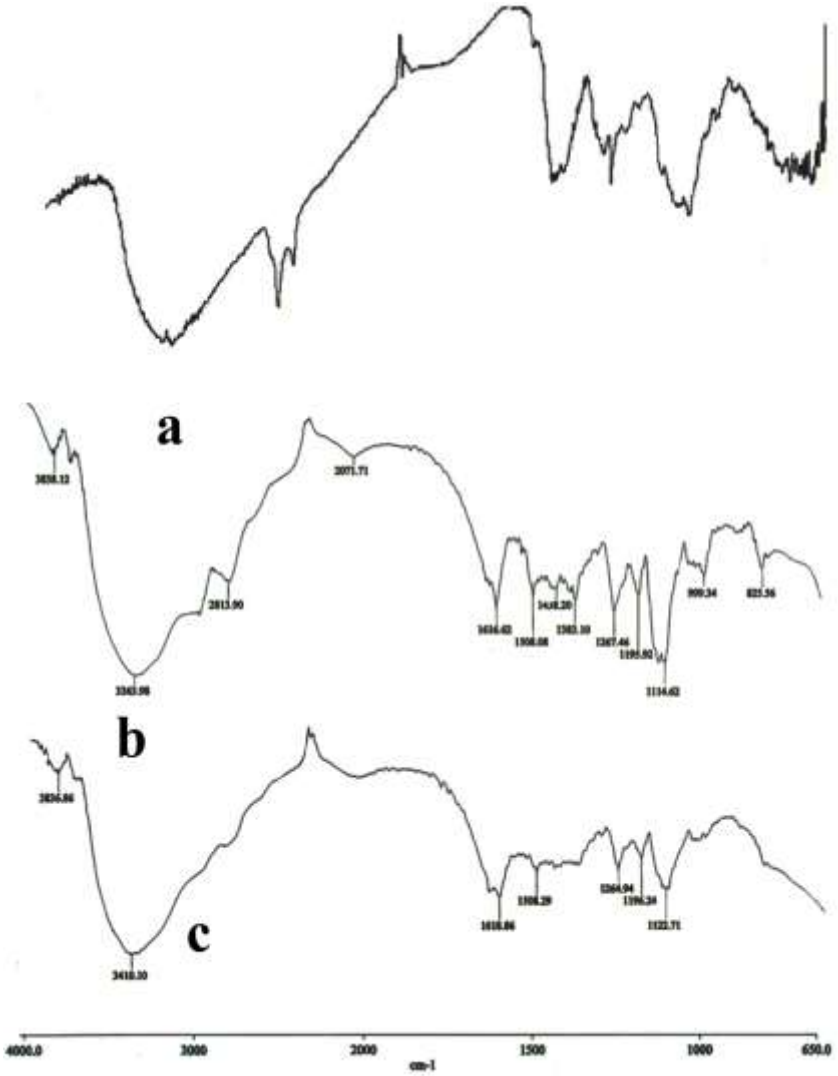

Figure 3. FTIR Spectra of Chitosan (a), Salbutamol sulphate (b) and microparticle (c).

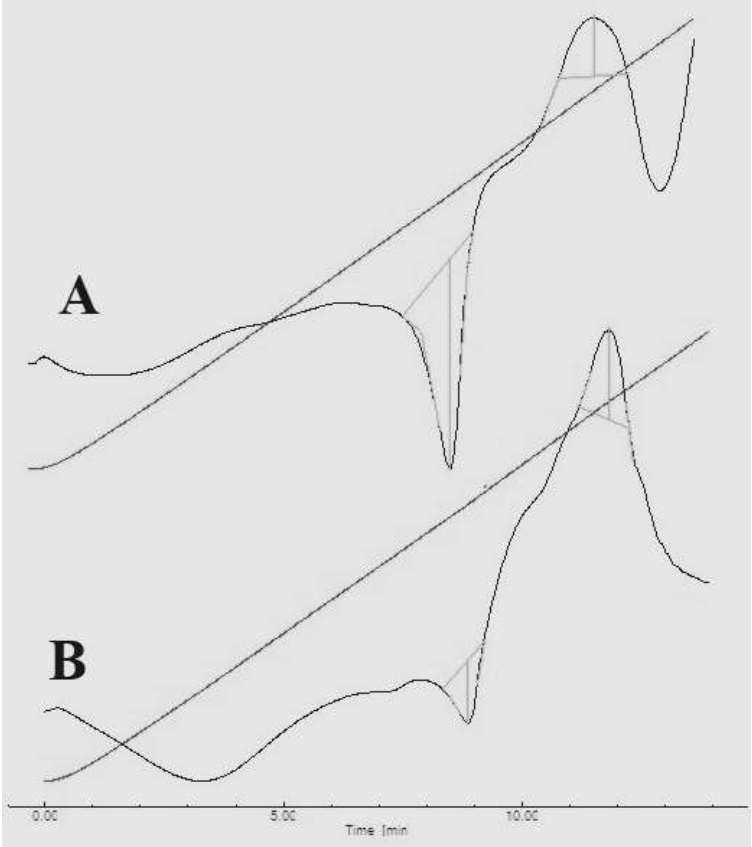

Figure 4. DSC thermogram (A- salbutamol and B-coated microparticle)

Swelling study

The swelling studies of the microsphere formulations (MSF-1 to MSF-8) over a 24-hour period reveal critical insights into their swelling behavior and equilibrium. Initially, all formulations exhibit rapid swelling within the first hour, with MSF-8 showing the highest swelling percentage of 550%, followed by MSF-7 at 500%, and MSF-5 at 400%. This trend suggests that higher polymer content significantly enhances the water absorption capacity of the microspheres. The formulations generally reach their maximum swelling between 5 to 6 hours, after which the swelling percentages stabilize. MSF-8 maintains the highest stable swelling percentage at 580%, while MSF-7 remains at 550%, indicating that these formulations achieve and maintain higher equilibrium swelling levels compared to others. Formulations MSF-1 to MSF-4, with a 1:1 drug-to-polymer ratio, show similar swelling behaviors, with maximum swelling percentages ranging from 360% to 380%, stabilizing after 5 hours. The variations in stirring speed for these formulations do not significantly affect their swelling capacities, suggesting that within the tested range, stirring speed is not a critical factor. In contrast, formulations MSF-5 to MSF-8, with higher polymer content, demonstrate significantly higher swelling percentages. For example, MSF-5 stabilizes at 450%, MSF-6 at 480%, MSF-7 at 550%, and MSF-8 at 580%. This indicates that higher polymer concentrations enhance the hydrophilicity and swelling capacity of the microspheres. Overall, the swelling behavior of the microsphere formulations is primarily influenced by the drug-to-polymer ratio and polymer type, with higher polymer content resulting in increased swelling capacity. All formulations reach equilibrium swelling between 5 to 6 hours, reflecting a rapid initial swelling phase followed by stabilization. These findings are crucial for optimizing the formulations for controlled drug delivery applications, ensuring that the microspheres exhibit the desired swelling characteristics for effective performance (Roy et al., 2009, Shivakumar et al., 2010).

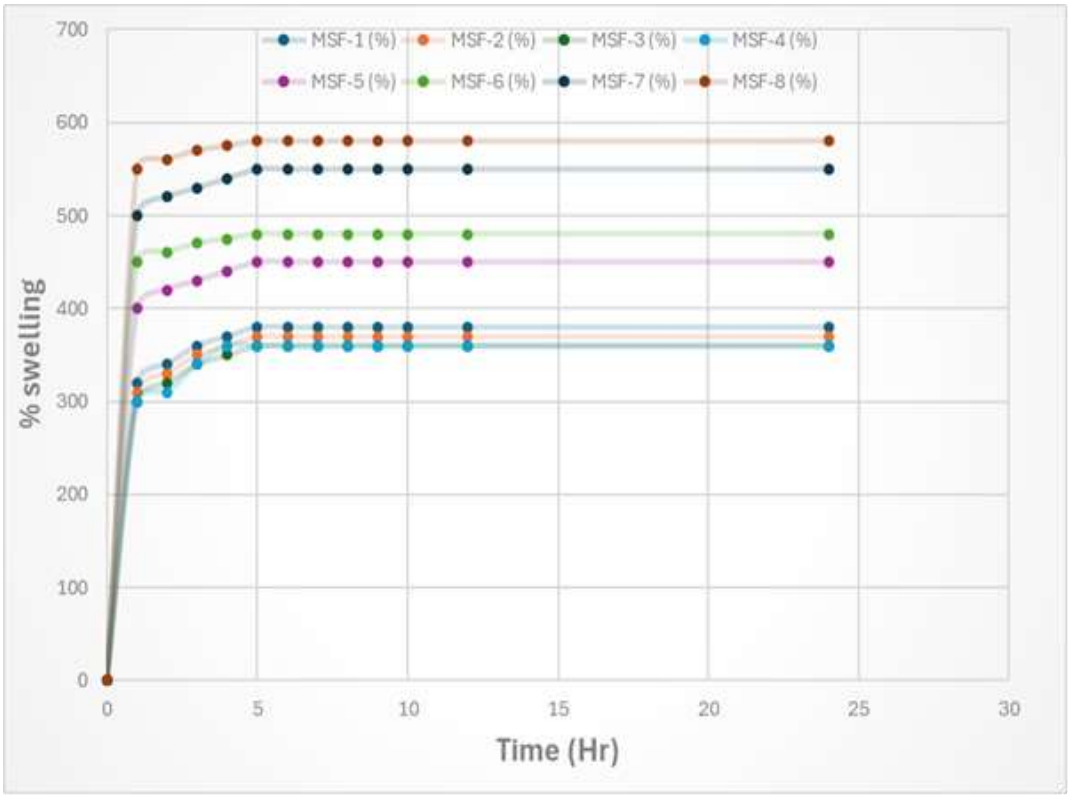

Figure 5. Swelling profile of core microparticle at pH 7

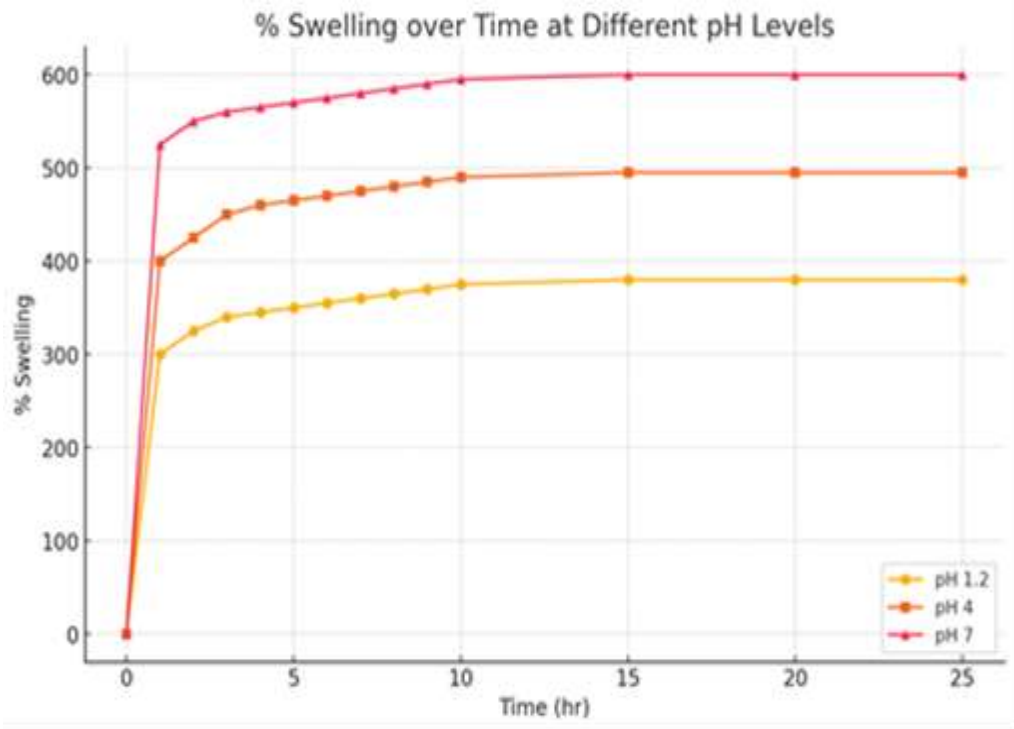

Figure 6. Swelling profile of MSF-3 at different pH (pH 1.2, pH 4 and pH 7).

Drug release from core microparticle

The drug release profiles of eight core microparticle formulations (MSF-1 to MSF-8) were evaluated at different pH levels: pH 1.2, pH 4.5, and pH 7.4. At pH 1.2 over a 2-hour period, the drug release ranged from 31.08% in MSF-8 to 53.08% in MSF-4, with MSF-4 showing the highest release. Similarly, at pH 4.5, MSF-4 again exhibited the highest release at 63.08%, whereas MSF-8 had the lowest release at 41.07%. When tested at pH 7.4 over 14 hours, the drug release was notably higher for all formulations compared to the acidic conditions. MSF-4 achieved the highest cumulative release of 118.087%, while MSF-8 had the lowest at 96.28%. The observations indicate that drug release was generally lower in acidic conditions, with a slightly higher release observed at pH 4.5 compared to pH 1.2. However, all formulations demonstrated significantly higher drug release at the neutral pH of 7.4, suggesting that a neutral environment facilitates more complete drug release over time. MSF-4 consistently showed the highest release across all pH levels, indicating a formulation less sensitive to pH variations and capable of rapid and sustained release. On the other hand, MSF-8 maintained the slowest release profile, making it suitable for sustained-release applications, particularly in neutral pH environments. These findings suggest that MSF-4 is ideal for conditions requiring rapid and complete drug release across various pH environments, making it versatile for diverse physiological conditions. Conversely, MSF-8, with its controlled and prolonged release, is better suited for sustained-release formulations. The results underscore the importance of tailoring formulations to specific therapeutic needs and environmental conditions to optimize drug delivery performance.

Drug release from coated microsphere

The drug release profiles of three coated microsphere formulations (EMC 1, EMC 2, and EMC 3) were examined over a 20-hour period, demonstrating distinct release behaviors aligned with the concept of enteric-coated chitosan microparticles. These microparticles are designed to prevent drug release in the stomach and upper intestinal pH, ensuring a rapid release in the lower intestinal pH, which proves their potential for chronotherapeutic drug delivery. For EMC 1, no drug release was observed for the first six hours, which corresponds to the pH conditions of the stomach and upper intestines. At the 7-hour mark, drug release began at 22%, increasing steadily to 43% at 8 hours and 53% at 9 hours. The release continued to rise, reaching 62% at 10 hours and 73% at 11 hours. By the 12th hour, the release was 83%, reaching near-complete release at 101% by the 14th hour, and stabilizing at 102% from the 15th hour onwards, with a slight fluctuation to 103% at the 19th hour. EMC 2 showed no drug release until the 7-hour mark, similar to EMC 1. At 7 hours, the release started at 12%, increasing to 22% at 8 hours and 33% at 9 hours. The drug release then followed a steady increase, reaching 42% at 10 hours, 53% at 11 hours, and 62% at 12 hours. By 13 hours, the release was 74%, and 81% at 14 hours. Complete release was achieved at 102% by the 16th hour, with minor fluctuations observed, reaching 103% at the 18th hour. In contrast, EMC 3 exhibited an earlier onset of drug release compared to EMC 1 and EMC 2. There was no release for the first hour, but by the second hour, the release began at 16%. The release increased to 19% at 3 hours and 26% at 4 hours. A more substantial increase was observed at 5 hours with 35%, and by 6 hours, the release reached 42%. From the 7th hour onwards, EMC 3 showed a rapid increase in drug release, reaching 62% at 7 hours, 82% at 8 hours, and 92% at 9 hours. The release peaked at 102% by the 10th hour and remained steady for the remainder of the observation period. These findings illustrate the effectiveness of enteric-coated chitosan microparticles in preventing drug release in the stomach and upper intestines while ensuring rapid release in the lower intestines. The varied release profiles among EMC 1, EMC 2, and EMC 3 highlight their suitability for different therapeutic needs. EMC 3 is particularly suitable for applications requiring rapid drug release in the lower intestines, while EMC 1 and EMC 2 are better suited for more controlled release scenarios. This targeted release mechanism confirms the potential of these microparticles for chronotherapeutic drug delivery, providing a promising system for timed and localized drug administration.

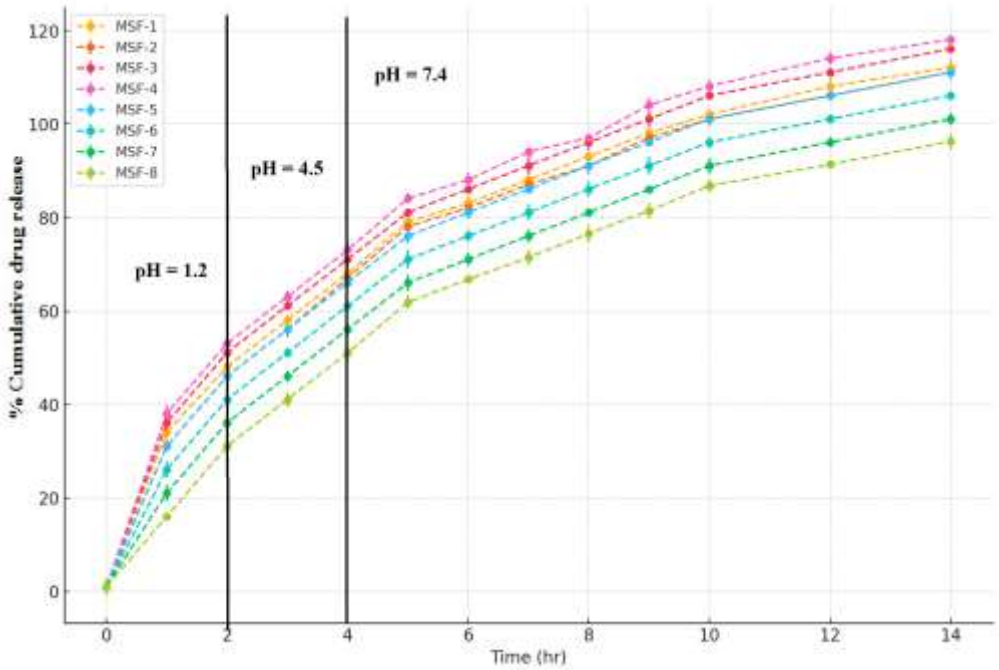

Figure 7. Drug release of different core microparticle at pH 1.2(2 hr),pH 4.5 (2 hr) and pH 7.4.

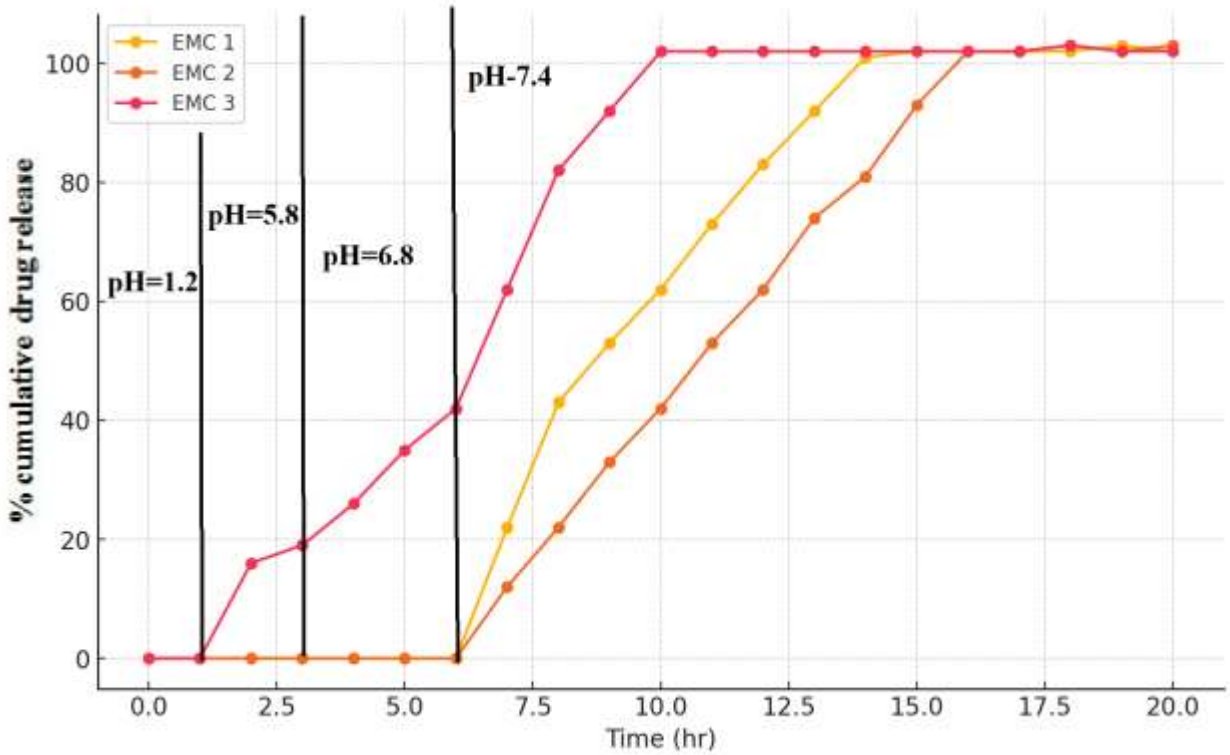

Figure 8. Drug release of different Coated microparticle at pH 1.2 (2 hr), pH 5.8 (2 hr), pH 6.8(2 hr) and pH 7.4.

Drug release Kinetics

The pharmacokinetic modeling of various formulations reveals distinct drug release profiles based on zero-order, first-order, Higuchi, and Korsmeyer-Peppas models. For the MSF formulations (MSF-1 to MSF-8), the zero-order model showed moderate fit with r2 values ranging from 0.8485 (MSF-4) to 0.9096 (MSF-

8). The zero-order rate constants (K0) were relatively consistent, with MSF-4 having the highest K0 of 7.2369. The first-order model generally showed lower r2 values compared to other models, indicating it is less suitable for describing the release kinetics of these formulations. However, MSF-7 and MSF-8 had exceptionally high r2 values (0.9978 and 0.9989), suggesting an atypical first-order release. The Higuchi model fit well across all MSF formulations, with r2 values around 0.99, suggesting diffusion-controlled release, and MSF-4 had the highest Kh of 34.4064. The Korsmeyer-Peppas model provided excellent fits with r2 values close to 0.99, and n values less than 0.5 for all formulations except MSF-7 and MSF-8, indicating Fickian diffusion. For the EMC formulations (EMC-1, EMC-2, and EMC-3), EMC-1 and EMC-2 showed moderate fits with the zero-order model ($r2 \approx 0.85$), with low K0 values suggesting a slower initial release rate. EMC-3 had the highest zero-order r2 value of 0.9322, indicating a consistent release rate with the highest K0 of 8.9560 among all formulations. The first-order model fit poorly for EMC-1 and EMC-2, with extremely low Kf values, indicating a non-first-order release mechanism, while EMC-3 had a higher r2 value of 0.9381, fitting the first-order model better than the others. The Higuchi model fit poorly for EMC-1 and EMC-2 ($r2 \approx 0.66$ and 0.64), indicating that the release is not purely diffusion-controlled, but EMC-3 showed a better fit with an r2 of 0.8636. The Korsmeyer-Peppas model revealed interesting insights, particularly for EMC-1 and EMC-2 with n values significantly greater than 1 (1.9080 and 2.1717), indicating super case-II transport mechanisms and suggesting that the enteric coating significantly impacts the release mechanism. EMC-3 had an n value close to 1, indicating a zero-order release mechanism. These results highlight the variability in drug release profiles, allowing for the selection of formulations based on desired release kinetics and therapeutic needs. MSF-4 stands out with high zero-order and Higuchi constants, indicating it is suitable for a consistent and diffusion-controlled release. EMC-3 shows excellent zero-order fit, suggesting it is ideal for sustained release applications. EMC-1 and EMC-2, with their complex release mechanisms, are promising for applications requiring controlled and delayed release, leveraging the benefits of enteric coating for chronotherapeutic drug delivery.

Table 4. Drug Release and kinetic of different formulation.

	Zero order		First Order		Higuchi		Pappas	
Formulation	**r2**	**K0**	**r2**	**Kf**	**r2**	**Kh**	**r2**	**n**
MSF-1	0.8589	6.9843	0.4712	33.1132	0.9892	32.4232	0.9940	0.4317
MSF-2	0.8631	7.0031	0.4534	30.4071	0.9885	31.9157	0.9918	0.4461
MSF-3	0.8554	7.1502	0.4819	35.5261	0.9893	33.5679	0.9954	0.4229
MSF-4	0.8485	7.2369	0.4924	37.4879	0.9873	34.4064	0.9951	0.4133
MSF-5	0.8711	7.0101	0.4509	30.3892	0.9916	31.7370	0.9941	0.4513
MSF-6	0.8859	6.8687	0.4183	25.1864	0.9920	29.9053	0.9924	0.4833
MSF-7	0.8996	6.7277	0.9978	0.1874	0.9900	28.0732	0.9901	0.5198
MSF-8	0.9096	6.6184	0.9989	0.1659	0.9841	26.3785	0.9856	0.5610
EMC 1	0.8592	6.9878	0.8592	0.00001	0.6612	13.5596	0.9109	1.9080
EMC 2	0.8521	4.9263	0.8521	0.000009	0.6359	9.1527	0.9416	2.1717
EMC 3	0.9322	8.9560	0.9381	0.0160	0.8636	24.9159	0.9320	1.0043

CONCLUSIONS

The study successfully developed and evaluated chitosan-based microparticles for controlled drug release, with salbutamol sulphate as the model drug. The core microparticles, synthesized using a w/o emulsion method and coated with eudragit, exhibited distinct morphological and release characteristics. The particle size and uniformity were influenced by stirring speed and drug-to-polymer ratios, while the coating significantly enhanced drug entrapment efficiency and yield. SEM analysis confirmed the structural integrity and surface morphology, while FTIR and DSC studies validated the chemical stability and compatibility of the formulations. Swelling studies indicated that higher polymer content resulted in increased water absorption, crucial for controlled release applications. Drug release studies revealed that the core microparticles had varied release profiles across different pH levels, with MSF-4 demonstrating the highest cumulative release and EMC-3 showing rapid release in lower intestinal pH, confirming their

potential for chronotherapeutic drug delivery. The pharmacokinetic modeling highlighted that MSF-4 and EMC-3 are suitable for consistent and sustained release applications, respectively. Overall, this research provides valuable insights into the formulation and optimization of chitosan-based microparticles, offering a promising approach for targeted and controlled drug delivery systems. Enteric coated chitosan microparticles leads to prevention of release in stomach pH and upper intestinal pH and rapid release of certain amount of drug on lower intestinal pH proved that it is a potential system for chronotherapeutic drug delivery.

REFERENCES

1. AODAH, A. H. Y. 2009. *Design and evaluation of Chronotherapeutic drug delivery Systems for the treatment of Nocturnal asthma*. Master Degree, King Saud University.
2. BOGIN, R. M. & BALLARD, R. D. 1992. Treatment of nocturnal asthma with pulsed release albuterol. *Chest,* 102**,** 362-366.
3. COCHRANE, G. M. & CLARK, T. J. H. 1975. A survey of asthma mortality in patients between 35 and 65 years in the greater London hospitals in 1971. *Thorax,* 30**,** 300-315.
4. DHAWAN, S., SINGLA, A. K. & SINHA, V. R. 2004. Evaluation of Mucoadhesive Properties of Chitosan Microspheres Prepared by Different Methods. *AAPS PharmSciTech,* 5**,** 1-7.
5. DUBEY, R. R. & PARIKH, R. H. 2004. Two-Stage Optimization Process for Formulation of Chitosan Microspheres. *AAPS PharmSciTech,* 5**,** 1-9.
6. GAO, J.-G., ZHANG, Y., YU, Y.-F., HAN, Y.-C., ZHANG, B.-Z. & GAO, C.-H. 2011. Preparation of chitosan microspheres loading of 3,5-dihydroxy-4-<i>i</i>-propylstilbene and in vitro release. *Journal of Polymer Research,* 18**,** 1501-1508.
7. JEYANTHI, R., MEHTA, R. C., THANOO, B. C. & DELUCA, P. P. 1997. Effect of processing parameters on the properties of peptide-containing PLGA microspheres. *J Microencapsul.,* 14**,** 163-174.
8. JOSE, S., PREMA, M. T., CHACKO, A. J., THOMAS, A. C. & SOUTO, E. B. 2011. Colon specific chitosan microspheres for chronotherapy of chronic stable angina. *Colloids and Surfaces B: Biointerfaces,* 83**,** 277-283.
9. KIKUCHI, A., KAWABUCHI, M., SUGIHARA, M., SAKURAI, Y. & OKANOA, T. 1999. Pulsed dextran release from calcium-alginate gel beads. *Journal of Controlled Release* 47**,** 21-29.
10. KIKUCHI, A. & OKANO, T. 2002. Pulsatile drug release control using hydrogels. *Adv. Drug Deliv. Rev.,* 54**,** 53-77.
11. LIU, F., LIU, L., XUEMIN, L. & ZHANG, Q. 2007. Preparation of chitosan-hyaluronate double-walled microspheres by emulsification-coacervation method. *J Mater Sci: Mater Med,* 18**,** 2215-2224.
12. LORENZO-LAMOSA, M. L., REMUN˜A´N-LO´PEZ, C., VILA-JATO, J. L. & ALONSO, M. L. 1998. Design of microencapsulated chitosan microspheres for colonic drug delivery. *Journal of Controlled Release,* 52**,** 109-118.
13. PACHUAU, L. & MAZUMDER, B. 2009. A study on the effects of different surfactants on thylcellulose microspheres. *International Journal of PharmTech Research,* 1**,** 966-971.
14. PATEL, G. C. & PATEL, M. M. 2009. A comparative in vitro evaluation of enteropolymers for pulsatile drug delivery system. *Acta Pharmaceutica Sciencia,* 51**,** 243- 250.
15. ROY, P. & SHAHIWALA, A. 2009. Statistical optimization of ranitidine HCl floating pulsatile delivery system for chronotherapy of nocturnal acid breakthrough. *European Journal of Pharmaceutical Sciences,* 37**,** 363-369.
16. ROY, S., PANPALIA, S. G., NANDY, B. C., RAI, V. K., TYAGI, L. K., DEY, S. & MEENA, K. C. 2009. Effect of Method of Preparation on Chiosan Microspheres of Mefenamic Acid. *International Journal of Pharmaceutical Sciences and Drug Research,* 1**,** 36-42.
17. SHIVAKUMAR, H. N., SURESH, S. & DESAI, B. G. 2010. Design and Evaluation of controlled Onset Extended Release Multiparticulate Systems for Chronotherpeutic Delivery of Ketoprofen. *J Mater Sci: Mater Med,* 21**,** 2691-2699.
18. SHUKLA, P. G., KALIDHASS, B., SHAH, A. & PALASHKAR, D. V. 2002. Preparation and characterization of microcapsules of water soluble pesticide monocrotophs using polyurethane as carrier material. *J Microencapsul.,* 19**,** 293-304.

19. SMOLENSKY, M. H., LEMMER, B. & REINBERG, A. E. 2007. Chronobiology and chronotherapy of allergic rhinitis and bronchial asthma. *Adv. Drug Deliv. Rev.,* 59**,** 852-882.
20. SONI, M. L., NAMDEO, K. P., JAIN, S. K., GUPTA, M., DANGI, J. S., KUMAR, M. & DANGI, Y. S. 2011. pH-Enzyme Di-dependent Chronotherapeutic Drug Delivery System of Theophylline for Nocturnal Asthma. *Chem.Pharm.Bull.,* 59**,** 191-195.
21. UMADEVI, S. K., THIRUGANESHA, R., SURESHA, S. & REDDYA, K. B. 2010. Formulation and Evaluation of Chitosan Microspheres of Aceclofenac for Colon-Targeted Drug Delivery. *Biopharm. Drug Dispos.,* 31**,** 407-427.
22. WARWICK, M. T. 1988. Epidemiology of nocturnal asthma. *Am. J. Med.,* 58**,** 6-8.
23. WILDING, R., DAVIS, S. S., POZZI, F., FURLANI, P. & GAZZANIGA, A. 1994. Enteric coated timed release system for colonic targeting. *Int. J. Pharm,* 111**,** 99-102.